



Published in final edited form as:

*Circ Heart Fail.* 2015 March ; 8(2): 362–372. doi:10.1161/CIRCHEARTFAILURE.114.001274.

## Loss of sFRP-1 Leads to Deterioration of Cardiac Function in Mice and Plays a Role in Human Cardiomyopathy

Piotr Sklepkiwicz, PhD<sup>1</sup>, Takayuki Shiomi, MD, PhD<sup>1</sup>, Rajbir Kaur, MS<sup>1</sup>, Jie Sun, MD<sup>1</sup>, Susan Kwon, MD<sup>1</sup>, Becky Mercer, PhD<sup>1</sup>, Peter Bodine, PhD<sup>2</sup>, Ralph Theo Schermuly, PhD<sup>3</sup>, Isaac George, MD<sup>5</sup>, P. Christian Schulze, MD, PhD<sup>4</sup>, and Jeanine M. D'Armiento, MD, PhD<sup>1</sup>

<sup>1</sup>Center for Molecular Pulmonary Disease, Department of Anesthesiology, College of Physicians and Surgeons, Columbia University, New York, NY

<sup>2</sup>Women's Health Research Institute, Wyeth Research, Collegeville, PA

<sup>3</sup>Max Planck Institute, Bad Nauheim, Germany

<sup>4</sup>Center for Advanced Cardiac Care, Columbia University Medical Center, New York, NY

<sup>5</sup>Division of Cardiothoracic Surgery, Department of Surgery, New York Presbyterian Hospital/ Columbia University Medical Center, New York, NY

### Abstract

**Background**—The Wnt/ $\beta$ -catenin signaling pathway plays a central role during cardiac development and has been implicated in cardiac remodeling and aging. However, the role of Wnt modulators in this process is unknown. In the present study, we examined the role of the Wnt signaling inhibitor sFRP-1 in aged wildtype and sFRP-1 deficient mice.

**Methods and Results**—sFRP-1 gene deletion mice were grossly normal with no difference in mortality but developed abnormal cardiac structure and dysfunction with progressive age. Ventricular dilation and hypertrophy in addition to deterioration of cardiac function and massive cardiac fibrosis, all features present in dilated cardiomyopathy was observed in the aged sFRP-1 KO mice when aged. Loss of sFRP-1 led to increased expression of Wnt ligands (Wnt1, 3, 7b, 16) and Wnt target genes (Wisp1, Lef1) in aged hearts, which correlated with increased protein levels of  $\beta$ -Catenin. Cardiac fibroblasts lacking endogenous sFRP-1 showed increased  $\alpha$ SMA expression, higher cell proliferation rates and increased collagen production consistent with the cardiac phenotype exhibited in aged sFRP-1 KO mice. The clinical relevance of these findings was supported by the demonstration of decreased sFRP-1 gene expression and increased Wisp-1 levels in the left ventricles of patients with ischemic dilated cardiomyopathy (ICM) and dilated cardiomyopathy (DCM).

**Conclusions**—This study identifies a novel role for sFRP-1 in age-related cardiac deterioration and fibrosis. Further exploration of this pathway will identify downstream molecules important in

---

**Correspondence to:** Jeanine D'Armiento, Center for Molecular Pulmonary Disease, Department of Anesthesiology, College of Physicians and Surgeons of Columbia University, 630 West 168<sup>th</sup> Street, New York, NY 10032, jmd12@cumc.columbia.edu, Phone: 212-305-3745, Fax: 212 305-5052.

**Disclosures**  
None.

these processes and also suggest the potential use of Wnt signaling agents as therapeutic targets for age-related cardiovascular disorders in humans.

### Keywords

heart; cardiac aging; fibrosis; Wnt signaling; dilated cardiomyopathy

Heart failure (HF) affects more than 4 million people in the United States and more than 400,000 new cases are diagnosed each year and despite recent advances in the management of heart failure, the incidence and prevalence continues to rise.<sup>1</sup> HF is the most common cause of hospitalization for patients older than 65 years. As the number of people over age 65 in North America is expected to double over the next 25 years, the burden of heart failure in the elderly will markedly increase.<sup>2</sup> The incidence of cardiovascular disease as well as the rate of cardiovascular morbidity and mortality increases exponentially in the elderly suggesting that age per se is a major risk factor for cardiovascular diseases.<sup>3</sup>

Cardiac aging is associated with left ventricular hypertrophy and fibrosis leading to diastolic dysfunction and heart failure.<sup>4</sup> The aging heart is characterized by morphological and structural changes that lead to a functional decline and diminished ability to meet increased demand. Extensive evidence, derived from both clinical and experimental studies suggests that the aging heart undergoes significant fibrotic remodeling. Increased fibrosis is a major determinant of myocardial stiffness, which together with impaired relaxation creates the basis for the development of diastolic dysfunction.<sup>5</sup> A common pathological feature of aged humans and rodents is dilated cardiomyopathy (DCM).<sup>6-9</sup> DCM is characterized by impaired myocardial contractility, ventricular dilation and replacement fibrosis that is a major determinant of myocardial stiffness, which together with impaired relaxation create the basis for the development of diastolic dysfunction.<sup>5, 10</sup>

Wnt-proteins are a family of secreted cysteine-rich glycosylated proteins that are implicated in a variety of modeling and remodeling processes including cell proliferation, differentiation, apoptosis, cellular polarity<sup>11-14</sup> and cellular senescence.<sup>15, 16</sup> There are 19 human Wnt genes, and Wnt proteins which have been grouped into two classes, the canonical and non-canonical Wnt pathways. Canonical Wnts stabilize intracellular  $\beta$ -catenin, allowing  $\beta$ -catenin to translocate into the nucleus and influence the association of transcription factors such as Tcf/LEF with transcriptional co-repressors to activate Wnt-dependent target genes.<sup>12, 17, 18</sup> Altered Wnt signaling is implicated in various disease processes and several studies have suggested that this pathway is involved in cardiovascular remodeling,<sup>11, 14</sup> cardiac hypertrophy<sup>19-24</sup> and myocardial aging<sup>16</sup> but evidence for a distinct role of Wnt inhibitors is less prevalent. Modulation of Wnt signaling through delivery of secreted frizzled-related proteins (sFRPs) was shown to be beneficial in improving cardiac structure and function post-myocardial infarction (MI) in rodents.<sup>25, 26</sup> In addition, sFRPs were shown to be important for apoptosis-mediated cell death and vascular cell proliferation *in vitro* and *in vivo*.<sup>27</sup> Of the five sFRPs, sFRP-1 is present during both cardiac development and adult life and is abundantly expressed in the mouse and human heart.<sup>18</sup> In the present study, the role of sFRP-1 on cardiovascular structure and function was

examined in the aging heart. Through the use of sFRP-1 gene deletion mice, this study identifies an important novel function of sFRP-1 in age-related cardiac remodeling.

## Methods

### Animal studies

The sFRP-1 KO mouse line was constructed by replacing 1176 bp of exon 1 with a LacZ/MC1-Neo selection cassette as described previously<sup>28, 29</sup>. Mice were analyzed over a time period of one year. Prior to sacrifice, hemodynamic and echocardiographic analysis was performed and post-sacrifice measurements of the wet heart weight to body weight and histological analysis were performed the various time points as described. All experiments were approved by the Institute for Animal Care and Use Committee at Columbia University.

### Human heart samples

Human heart specimens were collected during the time of left ventricular assist device implantation and explantation at Columbia University Medical Center (New York, NY) under institutional guidelines. Non-diseased myocardium was obtained from human hearts that could not be used for cardiac transplantation. The study protocol was approved by the Institutional Review Board at Columbia University Medical Center and written and informed consent was obtained from all subjects.

### Echocardiographic analysis

Anesthetized animals were placed on a mouse bed in a shallow left lateral decubitus position. Transthoracic echocardiography was performed as previously described<sup>30</sup> using a pediatric broad band 6–15 MHz linear array ultrasound transducer (Agilent Sonas 5500; Agilent Technologies, Palo Alto, USA). The ultrasound beam depth was set at 2 cm and frame rate at 150 frames/s. The two dimensional parasternal short-axis views were obtained at the level of the LV papillary muscles.

### Hemodynamic analysis

*In vivo* intraventricular hemodynamic analysis was performed as previously described<sup>30</sup> on sFRP-1 KO and WT littermate mice at 6 and 12 months of age. A total of 21 mice (6 months: 4 wild-type and 6 knock-out mice; and 12 months: 4 wild-type and 7 knock-out mice) were anesthetized with 2.5% Avertin at 0.015 mL/g body weight. A midline incision in the neck exposed the trachea, and the mouse was intubated intratracheally with a 22-gauge angiocatheter (Becton Dickinson, Franklin Lakes, USA) which was secured with 3-0 silk suture USSC, Princeton, USA). Mice were mechanically ventilated with a 0.5 ml ambient air tidal volume at 110 breaths/min using a small animal respirator/ventilator (Columbus Instruments, Columbus, USA). A median sternotomy was performed, and the heart was exposed. Digitized intraventricular hemodynamic measurements were obtained via a left ventricle apical puncture with a 26-gauge fluid-filled angiocatheter (Becton Dickinson) attached to a high-fidelity pressure transducer that was connected to an eight-channel chart recorder set at 1,000 Hz (MacLab 8s; ADInstruments, Mountain View, USA). The data were stored on a computer for subsequent analysis (PowerMac 5300C; Apple Computer Inc., Cupertino, USA).

## Histological analysis

Hearts were arrested in diastole with PBS/20 mM KCl solution and pressure fixed at 20 mmHg with 10% neutral buffered formalin. Paraffin-embedded tissues were sectioned (6- $\mu$ m thick) and stained with hematoxylin and eosin. Masson's trichrome staining was performed to evaluate the myocardial collagen content and distribution.

## Immunohistochemistry

Sections were incubated 45 minutes at 65°C and subsequently deparaffinized in xylene. Slides were then hydrated with 100% to 80% ethanol and washed with running tap water. After antigen retrieval, sections were incubated in 3% hydrogen peroxide, washed and blocked for 30 minutes in 2% bovine serum albumin and probed overnight in 4°C with sFRP-1 (Abcam, 1:100) or Connexin 43 (Cell Signaling, 1:100) primary antibodies in (1:100). Biotinylated anti-rabbit secondary antibody and HRP-streptavidin enzyme conjugate were added and sections were incubated for 1h at room temperature and subsequently washed with PBS. Signal was detected by incubation with AEC substrate (Histostain SP Rabbit Primary AEC Kit (ZYMED Laboratories) and counterstained with hematoxylin and further analyzed by light microscope. For immunohistofluorescence analysis, sections were probed overnight at 4°C with  $\beta$ -catenin primary antibody (1:100 dilution). Subsequently sections were incubated with fluorescent Alexaflur anti-rabbit 488 secondary antibody (1:500 dilution).  $\beta$ -catenin and DAPI (1:1000 dilution) fluorescent signals were visualized by fluorescence microscopy.

## Pathway-Focused gene expression profiling using Real-Time PCR

Total RNA was isolated from tissue heart homogenates from sFPR-1 WT (n=3) versus KO (n=3) mice at one year of age with Qiagen RNeasy Mini Kit following the manufacturer's protocols. Quantity and quality of extracted RNA was determined by Nano Drop (Fisher). cDNA was prepared using RT2 Profiler First strand Kit (SABiosciences) according to protocol, which was then used to perform Wnt signaling mouse PCR Array with RT2 Profiler PCR Array system (SABiosciences) according to manufacturer's protocol. Real-Time PCR reaction was performed (Applied Biosystems) and further analyzed on the SABiosciences website according to the provided instructions.

## mRNA analysis by Real-Time PCR

Total RNA was isolated from tissue heart homogenates from sFPR-1 WT (n=5) versus KO (n=5) mice at 3, 6 and 12 months of age with Qiagen RNeasy Mini Kit with on column DNase digestion following the manufacturer's protocols. Quantity and quality of extracted RNA was determined utilizing Nano Drop (Fisher). cDNA was prepared using High Capacity cDNA Reverse Transcription Kit (ABI) according to protocol, which was then used to perform Real-Time PCR reaction with Taqman Gene expression master (ABI). Taqman probes were used against Wnt1, Wnt3, Wnt3, Wnt5a, Kremen1, Wnt16, Lef1,  $\beta$ -catenin and Wisp1 (all from ABI) and the results are presented as fold of regulation as compared to the housekeeping control gene  $\beta$ -Actin.

### Western blot analysis

Protein samples were prepared by homogenizing whole hearts extracted from sFRP-1 KO mice and WT littermates at one year of age. Each 50mg of heart tissue sample was lysed in 500µl of protein RIPA lysis buffer (Santa Cruz Biotechnology) and centrifuged. Tissue lysates were equalized and separated by electrophoresis using a 10% polyacrylamide gel, then transferred for 1h to nitrocellulose membranes (Bio-Rad). Membranes were blocked 1h in non-fat milk (5%). After blocking membranes were probed with primary antibodies in dilutions as follows:  $\beta$ -Catenin, (1:1000, Cell Signaling Technology),  $\alpha$ -Smooth Muscle Actin (1:1000, Abcam) and  $\beta$ -Actin (1:1000, Santa Cruz Biotechnology). Primary antibody binding was detected by HRP-conjugated secondary antibodies and enhanced chemiluminescence reagents (Pierce).

### Primary cardiac fibroblasts isolation and culture

Cardiac fibroblasts were isolated by enzymatic digestion using collagenase [1 mg/ml (Roche Applied Science, Indianapolis, IN) in HBSS including calcium and magnesium. Briefly, hearts were washed with PBS and dissected free of vessels and atria, washed in isolation media (DMEM, 20% FBS, 10% streptomycin/penicillin). The hearts were transferred to 50 ml falcon tubes quickly minced into very small pieces, and incubated at 37°C for 25 min under vigorous stirring. Using a 30 ml syringe attached firmly to the 6" long 14 gauge metal cannula the suspension was mixed up to 12 times, taking care to avoid frothing. After chunks settled the suspension was passed through the strainer (70µm pore size followed by 40µm pore size) into a 50ml tube. The cell suspension was spun down at 400g for 8min in 4C and plated on a T75 tissue-culture flask in culture medium [DMEM/Glutamax, 10% FBS, 5%, streptomycin/penicillin] and maintained in a humidified atmosphere of 5% CO<sub>2</sub> at 37°C. After overnight incubation, non-adherent cells were removed and adherent cells were further cultivated.

### Collagen assay

Primary cardiac fibroblasts isolated from the hearts of 3 months old sFRP-1 KO and WT littermate mice were plated in equal amounts (300,000 cells per T75) and cultured as described above without FBS. Culture media was collected from sFRP-1 KO and WT cardiac fibroblast at passage 2. To quantify collagen production in the media of sFRP-1 KO and WT cardiac fibroblasts, a Sircol Collagen assay was performed and used according to the manufacturer's protocol.

### Proliferation assay

For assessment of cellular proliferation, mouse cardiac fibroblasts from passage 2 were seeded in 48-well plates. Primary cells cultured in no serum conditions were pulsed with 1.5 µCi per well [<sup>3</sup>H] thymidine (Amersham Pharmacia Biotech Ltd). The [<sup>3</sup>H] thymidine content of cell lysates was determined by scintillation counting as described previously<sup>31</sup>.

### Statistical Analysis

Data are expressed as mean  $\pm$  SEM. We tested for the equal variances prior to all our t-test and ANOVA analysis with f test (for t test) or Levine's test (for ANOVA). Two-group

analysis was performed by Student's t-test with equal variances in all cases except in the Wnt5a comparison where variances were unequal. In the case of unequal variance two-group analysis was performed by Student's t-test with unequal variances. For the comparison of sFRP levels in the mouse and human heart the sample sizes were unequal and the differences between the three groups were compared by an analysis of variance (ANOVA) followed by Tukey-Kramer post test for unequal sample size. Two-sided P values < 0.05 were considered statistically significant. Statistical analysis for the Wnt-gene array (was performed in a Sabiosciences web-based software automatically after input of the raw data (<http://pcrdataanalysis.sabiosciences.com/pcr/arrayanalysis.php>)). Western blot quantification statistics were performed with the use of Kodak software. All the graphs were generated in Graph Pad Prism 6 software.

## Results

### Pattern of sFRP-1 expression in the myocardium

sFRP-1 was abundantly present in the mouse hearts at 3 (Figure 1A), 6 and 12 months of age in the WT hearts as detected by immunohistochemistry. In addition mRNA expression of sFRP-1 confirmed the abundance of sFRP-1 in the 3, 6 and 12 month old WT hearts (Figure 1B) and exhibited the age related increase in expression.

### Loss of sFRP-1 increases cardiac size

The cardiac phenotype of sFRP-1 KO mice compared to WT littermate controls was characterized over the course of one year (Figure 2). The sFRP-1 KO mice appeared normal at birth and at 3 months of age. While there was no significant difference in survival at one year of age, sFRP-1 KO mice exhibited a marked increase in heart size (Figure 2A) as compared to WT mice. At 6 months of age sFRP-1 KO mice developed cardiac hypertrophy when compared to WT littermates as shown by an increased heart/body weight ratio, which further progressed at one year of age (Figure 2B, n=5).

### Loss of sFRP-1 leads to cardiac remodeling with impaired cardiac function

Although little or no changes were detected in heart function at 3 and 6 months of age, at the one-year time-point sFRP-1 KO mice developed significant changes in cardiac structure and function. Histological analysis using H&E staining of the sFRP-1 KO hearts revealed mild hypertrophy and ventricular dilation compared to WT hearts (Figure 3A) at one year of age. Echocardiographic analysis of one-year old littermates confirmed that the sFRP-1 KO mice developed LV chamber dilation compared to WT mice (LV end diastolic dimension-LVEDD, Figure 3B) with an increase in LV posterior wall thickness (PW, Figure 3C) above the dilatation seen already at 6 months of age (Figure 3B). The increase in LV wall thickness was sustained at 12 months of age (Figure 3C). A significant decrease in fractional shortening (FS, Figure 3D) represents a decrease in the LV contractility in the sFRP-1 KO mice at one year of age. Furthermore, hemodynamic analysis of sFRP-1 KO hearts at one year of age revealed significant worsening of LV systolic functional parameters (Figure 4A-B) such as left ventricular systolic pressure (LVSP, Figure 4A) and LV dP/dT max (Figure 4B). Additionally, the diastolic functional parameters (Figure 4C-D) of sFRP-1 KO mice were decreased such as left ventricular end-diastolic pressure (LVEDP, Figure 4C) and

dP/dT peak negative (dP/dT min, Figure 4D). In addition, supporting the deterioration of cardiac function in aged sFRP-1 KO mice, we observed age-dependent downregulation of connexin 43 (Cx43) (Figure 4E). Gap junction channels composed of Cx43 are essential for normal heart formation and function<sup>32</sup> and this age dependent decrease in Cx43 in the sFRP-1 knockout heart is in line with the cardiac deterioration observed in the aged sFRP-1 KO mice. The heart rates for the animals during hemodynamic and echocardiographic analysis were not different between wildtype and knockout and ranged from 446 bpm; SD=61.9 in WT and 479 bpm; SD=52.32 in the KO.

### **Loss of sFRP-1 leads to abnormal Wnt/ $\beta$ -catenin signaling in the aging heart**

To determine whether the canonical Wnt signaling pathway mediated through  $\beta$ -catenin was disrupted in sFRP-1 KO mice, mRNA abundance of Wnt ligands was examined in aged sFRP-1 KO hearts (Figure 5). Interestingly, the main ligands responsible for inducing the canonical Wnt signaling pathway and targets of sFRP-1 for inhibition are significantly induced such as Wnt1, Wnt3 and Wnt7b (Figure 5A-C). In addition we observed suppression of Kremen1 (Wnt signaling antagonist, Figure 5D) and Wnt5a (non-canonical Wnt ligand, Figure 5E). Interestingly Wnt16, the aging and senescence marker, was upregulated in aged sFRP-1 KO (Figure 5F).

Next, the expression level of  $\beta$ -catenin in sFRP-1 KO hearts at 6 and 12 months of age (Figure 6A-B) was determined. As expected, a significant increase in the protein level of  $\beta$ -catenin in total heart homogenates of sFRP-1 KO hearts at 6 months of age (Figure 6A) was sustained until 12 months of age (Figure 6B) as compared to the hearts of their WT littermates. To further localize  $\beta$ -catenin protein, an immunohistofluorescent study was performed. We observed a uniform increase of  $\beta$ -catenin throughout the myocardium with increased localization to the cells membrane in the myocardium of the sFRP-1 KO hearts at 6 months as well as at 12 months of age (Figure 6C) as compared to their WT littermates, consistent with western blot analysis.

We did not detect significant changes in mRNA expression of  $\beta$ -catenin at 12 months (Figure 6D) of age but did demonstrate the upregulation of Lef1 in the sFRP-1 KO hearts at 12 months of age (Figure 6E), which is a prominent target of Wnt/ $\beta$ -catenin signaling pathway, all together suggesting that the canonical Wnt signaling pathway is operative in aged sFRP-KO hearts at 12 months of age. Additionally, the accumulation of  $\beta$ -catenin in the cell membrane of intercalated disks of the myocardium of the sFRP-1 KO hearts at one year of age is likely to contribute to the increase in wall stiffness in the sFRP-1 KO hearts.

### **Loss of sFRP-1 leads to increased cardiac fibrosis in aged mice**

Trichrome staining was performed on the histological sections of the hearts at the 6 and 12 months time point. A slight increase in development of fibrosis was observed in the sFRP-1 KO mice at 6 months (Figure 7A) of age; however, by 12 months of age, a massive increase in interstitial and perivascular fibrosis was noted in the sFRP-1 KO hearts compared with hearts from WT littermates (Figure 7A). These results together with the above mentioned hemodynamic observations suggest that sFRP-1 plays an important role in maintaining normal cardiovascular structure and function during aging and that the loss of sFRP-1 leads

to the development of fibrotic cardiac remodeling with deterioration of cardiac function in the aged mice.

The increase in fibrosis development in aged sFRP-1 KO hearts coincides with the enrichment of the sFRP-1 KO heart with canonical Wnt ligands such as Wnt1. The main profibrotic Wnt1 target gene, Wnt1-inducible signaling protein 1 (Wisp1), which has previously been shown to be involved in fibrosis development in the lung and heart is age-dependently up regulated in the sFRP-1 KO hearts at 6 and 12 months of age as compared to their WT littermates (Figure 7B). In addition to increased fibrosis in the hearts of sFRP-1 KO mice accompanied by significant upregulation of Wisp1, the treatment of cardiac fibroblast for 24h with Wisp1 was able to induce collagen 1 and 3 expression in the primary cardiac fibroblast isolated from WT mice (Figure 7C). We hypothesized that the loss of sFRP-1 in the heart regulated collagen production as well as the activation of cardiac fibroblasts. To test this hypothesis primary murine cardiac fibroblasts were isolated from sFRP-1 KO and WT mice and collagen production and proliferation capacity was measured. As expected, sFRP-1 was completely absent in the sFRP-1 KO cardiac fibroblasts (Figure 7D). Cardiac fibroblasts isolated from sFRP-1 KO hearts displayed a significant increase in collagen production (Figure 7E) and proliferation capacity (Figure 7F). Most interestingly, a significant increase in protein expression of  $\alpha$  smooth muscle actin was observed (Figure 7G-H) in cardiac fibroblasts isolated from sFRP-1 KO hearts as compared to WT cardiac fibroblasts.

### Loss of sFRP-1 and increased Wisp1 in human cardiomyopathy

To evaluate the relevance of the proposed hypothesis in human diseased hearts, gene expression analysis was performed on left ventricles (LV) from healthy (n=8), dilated cardiomyopathy (n=8) and ischemic dilated cardiomyopathy (n=7) patients. Interestingly, we observed that sFRP-1 gene expression was significantly suppressed in LVs of cardiomyopathic patients suggesting that loss of sFRP-1 correlates with cardiomyopathic changes also in the human hearts (Figure 8A). In addition, induction of Wisp1 as shown in the myocardium of sFRP-1 deficient mice at 12 month of age was also found in human cardiomyopathic hearts (Figure 8B) suggesting that Wnt signaling is operative in human cardiac failure suggesting that suppression of sFRP-1 might be crucial player in this process.

## Discussion

The present study identifies a novel role for sFRP-1, an endogenous inhibitor of the Wnt signaling pathway in an animal model of cardiac failure and human cardiomyopathies demonstrating that patients with this disease exhibit decreased levels of sFRP in their heart. Additionally, the experiments directly demonstrate that loss of sFRP-1 results in cardiac dilatation, myocardial fibrosis with deterioration of cardiac function and increased left ventricular end diastolic pressure characteristic of dilated cardiomyopathy. These structural changes are accompanied by an age-dependent increase in the expression of the canonical Wnt ligands,  $\beta$ -catenin protein levels and mRNA levels of Wnt target genes such as Lef1, age-related Wnt16 and profibrotic Wisp1. In addition, the loss of endogenous sFRP-1 in cardiac fibroblasts led to increased  $\alpha$ -SMA expression and collagen production as compared

to WT cardiac fibroblasts. Taken together, this data suggests that the loss of sFRP-1 and the subsequent increase in canonical Wnt signaling leads to an age-dependent impairment of cardiac function and progressive cardiac fibrosis.

Global overexpression of sFRP-1 post-MI improves cardiac function and reduces infarct size and rupture<sup>25</sup>. However, studies using a cardiac conditional transgenic mouse expressing sFRP-1 specifically in cardiomyocytes reported a larger infarct size and diminished cardiac function in transgenic mice compared to control littermates during ischemic preconditioning<sup>33</sup>. The difference between these two findings is potentially secondary to the tissue expression pattern of the transgene. In our present study, loss of sFRP-1 led first to mild cardiac hypertrophy and subsequently to cardiac fibrosis and deterioration of heart function as the mice aged. The disruption of cardiac function was associated with a decrease in connexin 43 (Cx43), which is a functional gap junction channel protein that positively correlates with normal cardiac function. A down regulation of cardiac Cx43 has been identified during normal cardiac development, cardiac aging<sup>34</sup> and in several cardiac disorders in mice and humans such as DCM or ICM<sup>32, 35-38</sup>. The fact that Cx43 is downregulated in the hearts of aged sFRP-1 deficient mice and that sFRP-1 gene expression is downregulated in the human hearts of DCM and ICM patients suggest that the cardiac phenotype observed in the aged sFRP-1 KO mice resembles human DCM.

The modulation of the Wnt/ $\beta$ -catenin signaling pathway is known to play a role in cardiac development and remodeling. The function of the downstream target of canonical Wnt signaling,  $\beta$ -catenin, depends on its subcellular localization. Membrane bound  $\beta$ -catenin maintains tissue architecture and cell polarity at adherens junctions by linking the cadherin cytoplasmic tail to the actin cytoskeleton<sup>20</sup>. In the presence of canonical Wnt signaling ligands,  $\beta$ -catenin is not targeted for proteosomal degradation and accumulates within the cell<sup>12, 13, 17</sup>. Cytoplasmic  $\beta$ -catenin translocates into the nucleus and forms a complex with transcription factors of the Tcf/Lef family and regulates expression of specific canonical Wnt signaling target genes such as Lef1, axin2, Wisp1 and also amplifies the Wnt signal by up regulating canonical Wnt ligands such as Wnt1<sup>12, 17, 23, 39-41</sup>. Both positive and negative Wnt signaling is observed during cardiac remodeling of the adult heart due to stress or injury; Wnt ligands, as well as frizzled-related proteins inhibiting Wnts, are expressed. Both  $\beta$ -catenin loss and gain of function mutations have been characterized<sup>42</sup> demonstrating that inhibition of canonical Wnt signaling by  $\beta$ -catenin loss attenuates LV remodeling and improves ventricular function<sup>19, 24, 42</sup>. Conversely, increased mortality, severely impaired fractional shortening and a phenotype of dilated cardiomyopathy were observed in  $\beta$ -catenin gain of function studies<sup>19, 24, 42</sup>. We demonstrate that indeed the phenotype observed in the sFRP-KO mice was accompanied by an increase in canonical Wnt ligand expression such as Wnt1, 3 and 7b known to promote  $\beta$ -catenin dependent transcriptional activity that was in line with age-related cardiac function impairment. In addition, a decrease in the non-canonical Wnt5a and canonical Wnt antagonist Kremen1 was seen. The Wnt signaling pathway is implicated in cellular senescence with Wnt16b as a marker of senescent cells<sup>15, 16</sup>. In the present study we observe the up regulation of Wnt16 in aged sFRP-1 KO hearts as compared to their WT littermates, which correlates with the accelerated cardiac aging phenotype observed.

The upregulation of canonical Wnt ligands correlates with the age-dependent increase in total  $\beta$ -catenin protein levels in heart homogenates of the sFRP-1 KO mice. Most importantly Lef1, a transcriptional target of the Wnt/ $\beta$ -catenin pathway was upregulated suggesting that the canonical Wnt pathway was operational in the aged hearts of the sFRP-1 KO mice. Since  $\beta$ -catenin accumulation in the cell membrane of cardiomyopathic hearts correlates with increased myocardial wall stiffness and left ventricular end diastolic pressure it is likely to be playing an important role in the maintenance of the cardiac structure and function as seen in aged sFRP-1 KO mice.

Progressive cardiac fibrosis as we saw in the sFRP-1 KO mice is a hallmark of aging<sup>16,43-45</sup> and associated with increased deposition of matrix proteins in the myocardium. Age-dependent accumulation of collagen in the heart leads to a progressive increase in ventricular stiffness and impaired diastolic function seen in DCM. The Wnt signaling pathway was previously connected with fibrosis during cardiac remodeling<sup>46, 47</sup> but its potential role in age-related cardiac fibrosis has not been defined. Interestingly RT-PCR based analysis performed on heart homogenates of sFRP-1 KO mice revealed upregulation of several Wnt target genes crucial for proliferation, cell growth and fibrosis. One of the most intriguing findings identified here is the age-dependent upregulation of Wisp1 in sFRP-1 KO hearts which was found to be critical in fibrotic processes in the lung<sup>48</sup> and the heart<sup>39, 41</sup> and is a prominent target gene of canonical Wnt signaling. Wisp1 was not only increased in the hearts of the sFRP-1 mice but incubation of primary cardiac fibroblast with Wisp1 increased collagen 1 and 3 production suggesting that loss of sFRP-1 modulates Wnt signaling molecules resulting in an increase in cardiac fibrosis and remodeling. A critical event in the development of cardiac fibrosis is the transformation of fibroblasts into an active fibroblast phenotype or myofibroblast<sup>49</sup>, characterized by the expression of contractile proteins, such as  $\alpha$  smooth muscle actin ( $\alpha$ SMA) and increased collagen production. We hypothesize that the cardiac fibrosis seen in the sFRP-1 KO correlates with activation of the fibroblast. Our *in vitro* results indicate that lack of endogenous sFRP-1 in primary cardiac fibroblasts potentially increases the susceptibility of these cells to differentiate into myofibroblasts, as represented by an increase in the expression of  $\alpha$  smooth muscle actin ( $\alpha$ SMA) and collagen production. In addition, the fact that we observed downregulation of sFRP-1 and upregulation of Wisp1 in human DCM and ICM suggests that the above described activation of Wnt signaling by loss of sFRP-1 might be crucial factor for development or acceleration of human cardiac disorders such as DCM or ICM.

This study suggests that the induction of the Wnt pathway is a potentially crucial pathway in the development of cardiomyopathy during aging with sFRP-1 being a critical factor in maintaining normal cardiovascular structure and function during this process. The cardiac phenotype represented in the mice lacking sFRP-1 provides us with novel insight into age-related cardiac function maintenance as still little is known of the molecular mechanisms prevent fibrosis and cardiac dysfunction in response to cumulative hemodynamic stress related to aging. Further studies elucidating the role of sFRP-1 in the heart and its regulation of the Wnt signaling pathway could help to understand the molecular mechanisms of cardiomyopathy and may support the potential clinical applications of new strategies to protect the heart during aging and disease.

## Acknowledgments

### Sources of Funding

This work was supported in part by NIH R01-HL086936 (J.M.D.), R01-HL100384 (J.M.D.) and Established Investigator Award-American Heart Association-0840108N (J.M.D.)

## References

1. Kannel WB. Incidence and epidemiology of heart failure. *Heart Fail Rev.* 2000; 5:167–173. [PubMed: 16228142]
2. Biernacka A, Frangiannis NG. Aging and cardiac fibrosis. *Aging Dis.* 2011; 2:158–173. [PubMed: 21837283]
3. Dai DF, Chen T, Johnson S, Szeto HH, Rabinovitch PS. Cardiac aging: From molecular mechanisms to significance in human health and disease. *Antioxid Redox Signal.* 2012; 16:1492–1526. [PubMed: 22229339]
4. Lakatta EG. Arterial and cardiac aging: Major shareholders in cardiovascular disease enterprises: Part iii: Cellular and molecular clues to heart and arterial aging. *Circulation.* 2003; 107:490–497. [PubMed: 12551876]
5. Burlew BS. Diastolic dysfunction in the elderly--the interstitial issue. *Am J Geriatr Cardiol.* 2004; 13:29–38. [PubMed: 14724399]
6. Coughlin SS, Tefft MC, Rice JC, Gerone JL, Baughman KL. Epidemiology of idiopathic dilated cardiomyopathy in the elderly: Pooled results from two case-control studies. *Am J Epidemiol.* 1996; 143:881–888. [PubMed: 8610701]
7. Harding P, Yang XP, Yang J, Shesely E, He Q, LaPointe MC. Gene expression profiling of dilated cardiomyopathy in older male ep4 knockout mice. *Am J Physiol Heart Circ Physiol.* 2010; 298:H623–632. [PubMed: 20008274]
8. Swinnen M, Vanhoutte D, Van Almen GC, Hamdani N, Schellings MW, D'Hooge J, Van der Velden J, Weaver MS, Sage EH, Bornstein P, Verheyen FK, VandenDriessche T, Chuah MK, Westermann D, Paulus WJ, Van de Werf F, Schroen B, Carmeliet P, Pinto YM, Heymans S. Absence of thrombospondin-2 causes age-related dilated cardiomyopathy. *Circulation.* 2009; 120:1585–1597. [PubMed: 19805649]
9. Lefta M, Campbell KS, Feng HZ, Jin JP, Esser KA. Development of dilated cardiomyopathy in bmal1-deficient mice. *Am J Physiol Heart Circ Physiol.* 2012; 303:H475–485. [PubMed: 22707558]
10. Towbin JA, Bowles NE. The failing heart. *Nature.* 2002; 415:227–233. [PubMed: 11805847]
11. Brade T, Manner J, Kuhl M. The role of wnt signalling in cardiac development and tissue remodelling in the mature heart. *Cardiovasc Res.* 2006; 72:198–209. [PubMed: 16860783]
12. Moon RT, Kohn AD, De Ferrari GV, Kaykas A. Wnt and beta-catenin signalling: Diseases and therapies. *Nat Rev Genet.* 2004; 5:691–701. [PubMed: 15372092]
13. Reya T, Clevers H. Wnt signalling in stem cells and cancer. *Nature.* 2005; 434:843–850. [PubMed: 15829953]
14. van Gijn ME, Daemen MJ, Smits JF, Blankesteyn WM. The wnt-frizzled cascade in cardiovascular disease. *Cardiovasc Res.* 2002; 55:16–24. [PubMed: 12062705]
15. Binet R, Ythier D, Robles AI, Collado M, Larrieu D, Fonti C, Brambilla E, Brambilla C, Serrano M, Harris CC, Pedeux R. Wnt16b is a new marker of cellular senescence that regulates p53 activity and the phosphoinositide 3-kinase/akt pathway. *Cancer Res.* 2009; 69:9183–9191. [PubMed: 19951988]
16. Naito AT, Shiojima I, Komuro I. Wnt signaling and aging-related heart disorders. *Circ Res.* 2010; 107:1295–1303. [PubMed: 21106946]
17. Huelsken J, Behrens J. The wnt signalling pathway. *J Cell Sci.* 2002; 115:3977–3978. [PubMed: 12356903]
18. Jones SE, Jomary C. Secreted frizzled-related proteins: Searching for relationships and patterns. *Bioessays.* 2002; 24:811–820. [PubMed: 12210517]

19. Baurand A, Zelarayan L, Betney R, Gehrke C, Dunger S, Noack C, Busjahn A, Huelsken J, Taketo MM, Birchmeier W, Dietz R, Bergmann MW. Beta-catenin downregulation is required for adaptive cardiac remodeling. *Circ Res.* 2007; 100:1353–1362. [PubMed: 17413044]
20. Hahn JY, Cho HJ, Bae JW, Yuk HS, Kim KI, Park KW, Koo BK, Chae IH, Shin CS, Oh BH, Choi YS, Park YB, Kim HS. Beta-catenin overexpression reduces myocardial infarct size through differential effects on cardiomyocytes and cardiac fibroblasts. *J Biol Chem.* 2006; 281:30979–30989. [PubMed: 16920707]
21. Haq S, Choukroun G, Kang ZB, Ranu H, Matsui T, Rosenzweig A, Molkenin JD, Alessandrini A, Woodgett J, Hajjar R, Michael A, Force T. Glycogen synthase kinase-3beta is a negative regulator of cardiomyocyte hypertrophy. *J Cell Biol.* 2000; 151:117–130. [PubMed: 11018058]
22. Masuelli L, Bei R, Sacchetti P, Scappaticci I, Francalanci P, Albonici L, Coletti A, Palumbo C, Minieri M, Fiaccavento R, Carotenuto F, Fantini C, Carosella L, Modesti A, Di Nardo P. Beta-catenin accumulates in intercalated disks of hypertrophic cardiomyopathic hearts. *Cardiovasc Res.* 2003; 60:376–387. [PubMed: 14613867]
23. Zelarayan L, Gehrke C, Bergmann MW. Role of beta-catenin in adult cardiac remodeling. *Cell Cycle.* 2007; 6:2120–2126. [PubMed: 17786052]
24. Zelarayan LC, Noack C, Sekkali B, Kmecova J, Gehrke C, Renger A, Zafiriou MP, van der Nagel R, Dietz R, de Windt LJ, Balligand JL, Bergmann MW. Beta-catenin downregulation attenuates ischemic cardiac remodeling through enhanced resident precursor cell differentiation. *Proc Natl Acad Sci U S A.* 2008; 105:19762–19767. [PubMed: 19073933]
25. Barandon L, Couffinhal T, Ezan J, Dufourcq P, Costet P, Alzieu P, Leroux L, Moreau C, Dare D, Duplaa C. Reduction of infarct size and prevention of cardiac rupture in transgenic mice overexpressing frza. *Circulation.* 2003; 108:2282–2289. [PubMed: 14581414]
26. He W, Zhang L, Ni A, Zhang Z, Mirosou M, Mao L, Pratt RE, Dzau VJ. Exogenously administered secreted frizzled related protein 2 (sfrp2) reduces fibrosis and improves cardiac function in a rat model of myocardial infarction. *Proc Natl Acad Sci U S A.* 2010; 107:21110–21115. [PubMed: 21078975]
27. Ezan J, Leroux L, Barandon L, Dufourcq P, Jaspard B, Moreau C, Allieres C, Daret D, Couffinhal T, Duplaa C. Frza/sfrp-1, a secreted antagonist of the wnt-frizzled pathway, controls vascular cell proliferation in vitro and in vivo. *Cardiovasc Res.* 2004; 63:731–738. [PubMed: 15306229]
28. Bodine PV, Zhao W, Kharode YP, Bex FJ, Lambert AJ, Goad MB, Gaur T, Stein GS, Lian JB, Komm BS. The wnt antagonist secreted frizzled-related protein-1 is a negative regulator of trabecular bone formation in adult mice. *Mol Endocrinol.* 2004; 18:1222–1237. [PubMed: 14976225]
29. Foronjy R, Imai K, Shiomi T, Mercer B, Sklepkiwicz P, Thankachen J, Bodine P, D'Armiento J. The divergent roles of secreted frizzled related protein-1 (sfrp1) in lung morphogenesis and emphysema. *Am J Pathol.* 2010; 177:598–607. [PubMed: 20595636]
30. Foronjy RF, Sun J, Lemaitre V, D'Armiento JM. Transgenic expression of matrix metalloproteinase-1 inhibits myocardial fibrosis and prevents the transition to heart failure in a pressure overload mouse model. *Hypertens Res.* 2008; 31:725–735. [PubMed: 18633185]
31. Sklepkiwicz P, Schermuly RT, Tian X, Ghofrani HA, Weissmann N, Sedding D, Kashour T, Seeger W, Grimminger F, Pullamsetti SS. Glycogen synthase kinase 3beta contributes to proliferation of arterial smooth muscle cells in pulmonary hypertension. *PLoS One.* 2011; 6:e18883. [PubMed: 21533110]
32. Bruce AF, Rothery S, Dupont E, Severs NJ. Gap junction remodelling in human heart failure is associated with increased interaction of connexin43 with zo-1. *Cardiovasc Res.* 2008; 77:757–765. [PubMed: 18056766]
33. Barandon L, Dufourcq P, Costet P, Moreau C, Allieres C, Daret D, Dos Santos P, Daniel Lamaziere JM, Couffinhal T, Duplaa C. Involvement of frza/sfrp-1 and the wnt/frizzled pathway in ischemic preconditioning. *Circ Res.* 2005; 96:1299–1306. [PubMed: 15920021]
34. Watanabe M, Ichinose S, Sunamori M. Age-related changes in gap junctional protein of the rat heart. *Exp Clin Cardiol.* 2004; 9:130–132. [PubMed: 19641700]
35. Roura S, Planas F, Prat-Vidal C, Leta R, Soler-Botija C, Carreras F, Llach A, Hove-Madsen L, Pons Llado G, Farre J, Cinca J, Bayes-Genis A. Idiopathic dilated cardiomyopathy exhibits

- defective vascularization and vessel formation. *Eur J Heart Fail.* 2007; 9:995–1002. [PubMed: 17719840]
36. Severs NJ, Bruce AF, Dupont E, Rothery S. Remodelling of gap junctions and connexin expression in diseased myocardium. *Cardiovasc Res.* 2008; 80:9–19. [PubMed: 18519446]
  37. Severs NJ, Dupont E, Thomas N, Kaba R, Rothery S, Jain R, Sharpey K, Fry CH. Alterations in cardiac connexin expression in cardiomyopathies. *Adv Cardiol.* 2006; 42:228–242. [PubMed: 16646594]
  38. Yoshida M, Ohkusa T, Nakashima T, Takanari H, Yano M, Takemura G, Honjo H, Kodama I, Mizukami Y, Matsuzaki M. Alterations in adhesion junction precede gap junction remodelling during the development of heart failure in cardiomyopathic hamsters. *Cardiovasc Res.* 2011; 92:95–105. [PubMed: 21693625]
  39. Colston JT, de la Rosa SD, Koehler M, Gonzales K, Mestril R, Freeman GL, Bailey SR, Chandrasekar B. Wnt-induced secreted protein-1 is a prohypertrophic and profibrotic growth factor. *Am J Physiol Heart Circ Physiol.* 2007; 293:H1839–1846. [PubMed: 17616748]
  40. Filali M, Cheng N, Abbott D, Leontiev V, Engelhardt JF. Wnt-3a/beta-catenin signaling induces transcription from the *lef-1* promoter. *J Biol Chem.* 2002; 277:33398–33410. [PubMed: 12052822]
  41. Venkatachalam K, Venkatesan B, Valente AJ, Melby PC, Nandish S, Reusch JE, Clark RA, Chandrasekar B. Wisp1, a pro-mitogenic, pro-survival factor, mediates tumor necrosis factor-alpha (tnf-alpha)-stimulated cardiac fibroblast proliferation but inhibits tnf-alpha-induced cardiomyocyte death. *J Biol Chem.* 2009; 284:14414–14427. [PubMed: 19339243]
  42. Bergmann MW. Wnt signaling in adult cardiac hypertrophy and remodeling: Lessons learned from cardiac development. *Circ Res.* 2010; 107:1198–1208. [PubMed: 21071717]
  43. Gagliano N, Arosio B, Santambrogio D, Balestrieri MR, Padoani G, Tagliabue J, Masson S, Vergani C, Annoni G. Age-dependent expression of fibrosis-related genes and collagen deposition in rat kidney cortex. *J Gerontol A Biol Sci Med Sci.* 2000; 55:B365–372. [PubMed: 10952357]
  44. Hinton DE, Williams WL. Hepatic fibrosis associated with aging in four stocks of mice. *J Gerontol.* 1968; 23:205–211. [PubMed: 5643886]
  45. Calabresi C, Arosio B, Galimberti L, Scanziani E, Bergottini R, Annoni G, Vergani C. Natural aging, expression of fibrosis-related genes and collagen deposition in rat lung. *Exp Gerontol.* 2007; 42:1003–1011. [PubMed: 17706388]
  46. Duan J, Gherghe C, Liu D, Hamlett E, Srikantha L, Rodgers L, Regan JN, Rojas M, Willis M, Leask A, Majesky M, Deb A. Wnt1/betacatenin injury response activates the epicardium and cardiac fibroblasts to promote cardiac repair. *Embo J.* 2012; 31:429–442. [PubMed: 22085926]
  47. Ye B, Ge Y, Perens G, Hong L, Xu H, Fishbein MC, Li F. Canonical wnt/beta-catenin signaling in epicardial fibrosis of failed pediatric heart allografts with diastolic dysfunction. *Cardiovasc Pathol.* 2012; 22:54–57. [PubMed: 22475572]
  48. Konigshoff M, Kramer M, Balsara N, Wilhelm J, Amarie OV, Jahn A, Rose F, Fink L, Seeger W, Schaefer L, Gunther A, Eickelberg O. Wnt1-inducible signaling protein-1 mediates pulmonary fibrosis in mice and is upregulated in humans with idiopathic pulmonary fibrosis. *J Clin Invest.* 2009; 119:772–787. [PubMed: 19287097]
  49. Brown RD, Ambler SK, Mitchell MD, Long CS. The cardiac fibroblast: Therapeutic target in myocardial remodeling and failure. *Annu Rev Pharmacol Toxicol.* 2005; 45:657–687. [PubMed: 15822192]

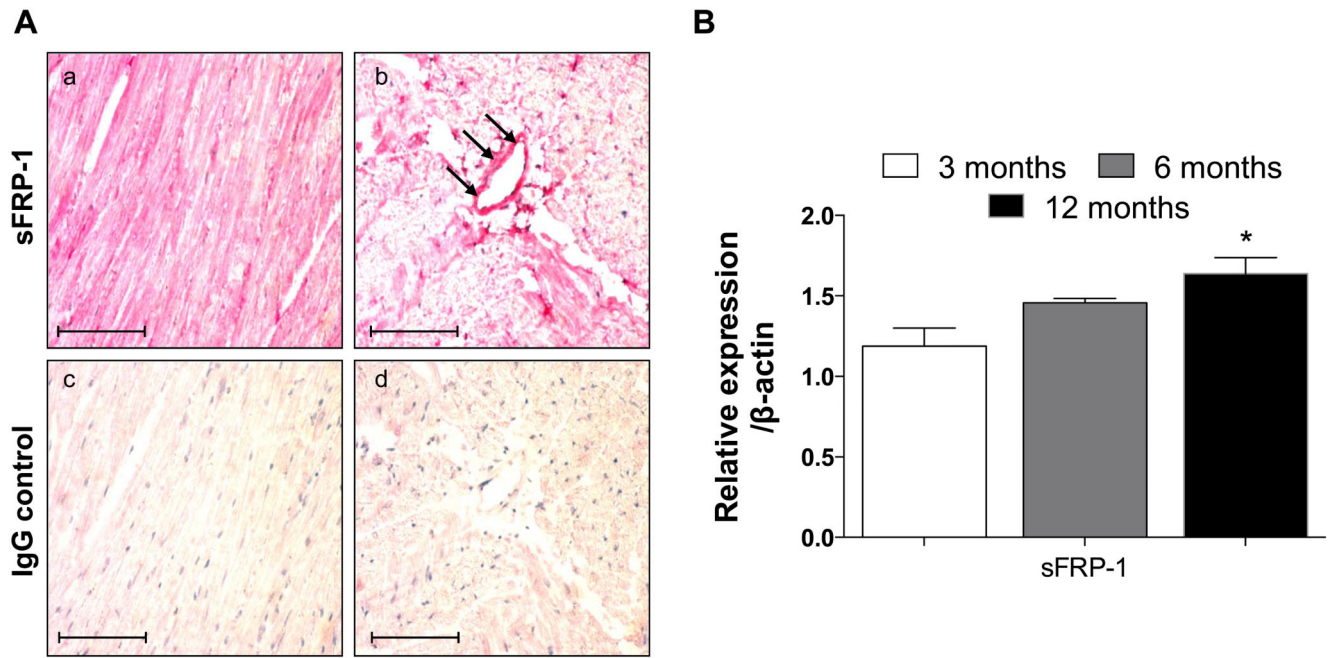


**Figure 1. Expression of sFRP-1 in the normal heart during aging**

(A) Immunohistochemical staining of sFRP-1 in heart sections of sFRP-1 WT mice at 3 months of age (a-b) with IgG controls (c-d). Sections were counterstained with hematoxylin. Magnification is 40 $\times$ . Scale bars represent length of 100 $\mu$ m. (B) mRNA expression of sFRP-1 in the hearts of sFRP-1 WT mice at 3, 6 (n=3) and 12 months of age (n=4) analyzed by RT-PCR with  $\beta$ -actin used as a housekeeping gene control. Data are presented as fold of regulation and statistically significant differences are denoted by \*p < 0.05.

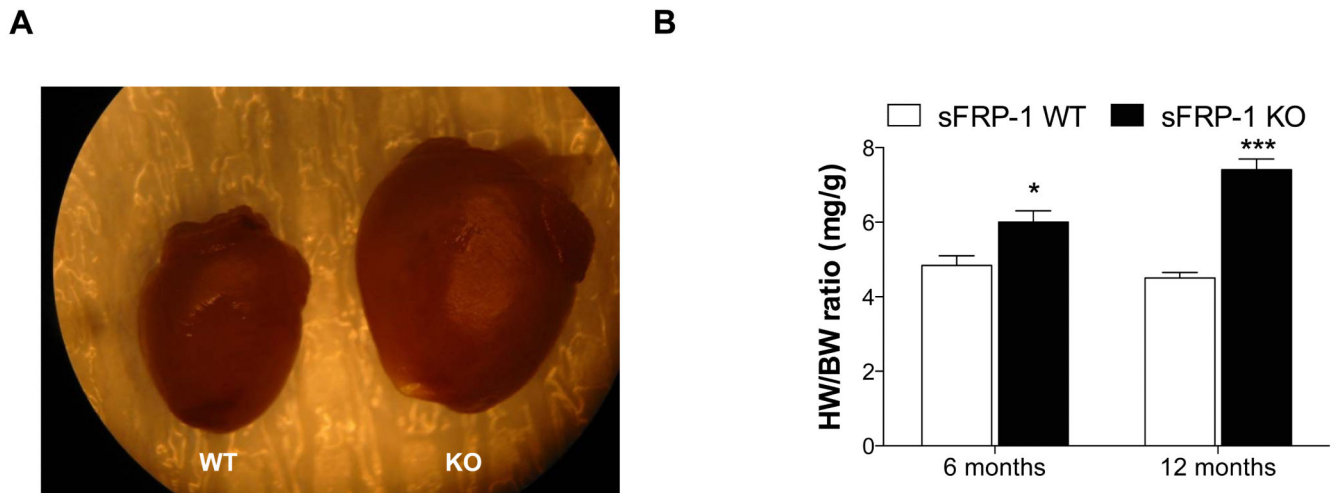


**Figure 2. Age-dependent increase in cardiac size in sFRP-1 KO mice**

(A) Representative picture from whole heart of WT and sFRP-1 KO mice at 12 months of age showing increase in heart size. (B) Heart weight/body weight ratio (mg/g) of the sFRP-1 KO mice at 6 months and 12 months of age (n=5) compared to their WT littermates. Significant differences were denoted by \* $P < 0.05$  or \*\* $P < 0.01$ , or \*\*\* $P < 0.001$ . > vs control littermate hearts. All values were expressed as mean  $\pm$  SEM.

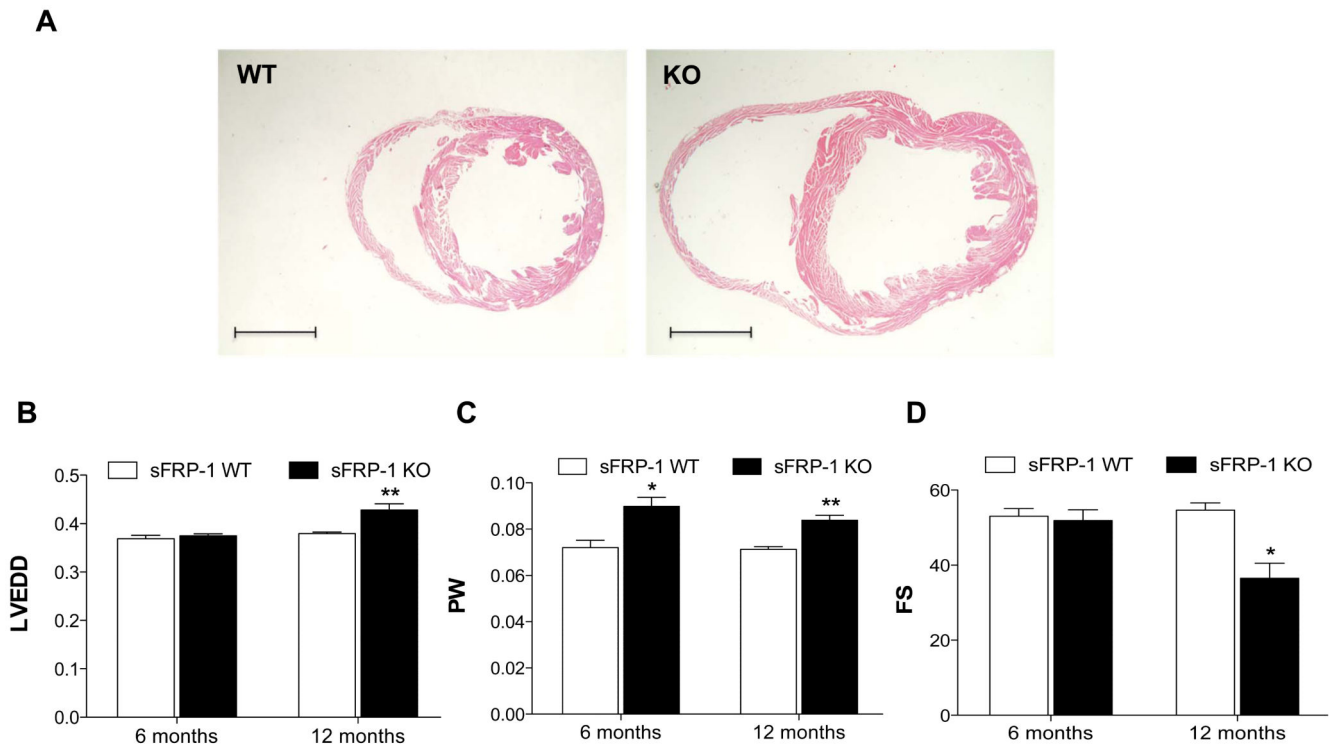


**Figure 3. Development of cardiac remodeling in aged sFRP-1 KO mice**

(A) Representative hematoxylin and eosin (H&E) staining of the sFRP-1 WT and sFRP-1 KO hearts at one year of age. Scale bars represent the length of 2mm. (B-D)

Echocardiographic analysis of the sFRP-1 WT and KO mice hearts representing (WT/n=3; KO/n=7); (B) LV end diastolic dimension (LVEDD- [cm]) (C) LV posterior wall thickness (PW-[cm]) (D) Fractional Shortening, (FS-[%]). Significant differences were denoted by \*P < 0.05 < \*\*P < 0.01, or \*\*\*P < 0.001. > vs control littermate hearts. All values were expressed as mean ± SEM

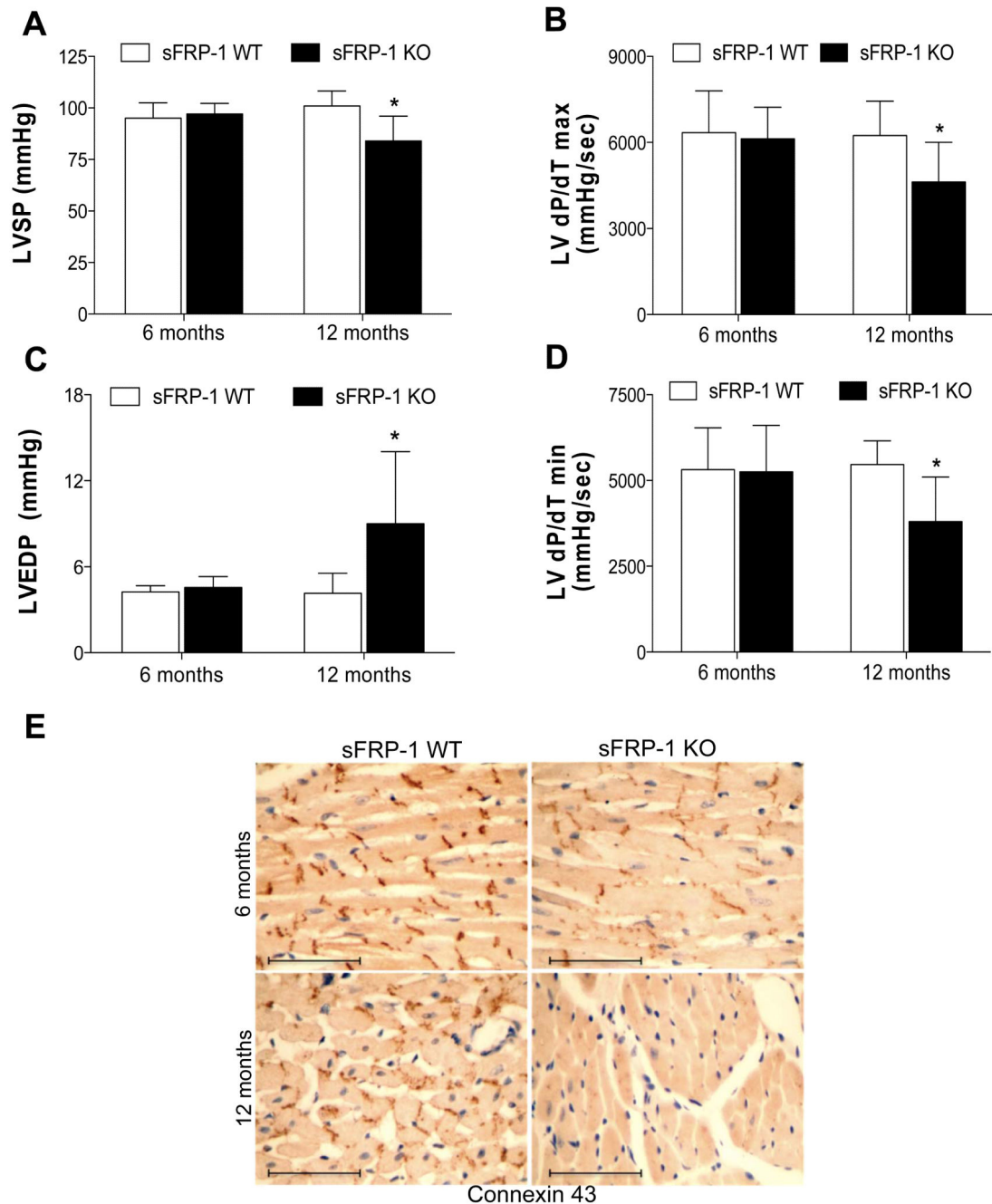


#### Figure 4. Deterioration of LV function in aged sFRP-1 KO mice

Hemodynamic analysis of LV systolic (A-B) and diastolic (C-D.) function in sFRP-1 KO mice compared to their WT littermates at 6 and 12 months of age (WT/n=4; KO/n=6) representing: (A) Left Ventricular Systolic Pressure (LVSP- [mmHg]), (B) dP/dT max [mmHg/sec], (C) Left Ventricular End Diastolic Pressure (LVEDP- [mmHg]), (D) dP/dT min [mmHg]- value as below 0. Significant differences were denoted by \*P < 0.05 < or \*\*P < 0.01, or \*\*\*P < 0.001. > vs control littermate hearts. All values were expressed as mean ± SEM, (E) Immunohistochemical staining of Connexin43 in heart sections at 6 months and

12 months of age. Sections were counterstained with hematoxylin. Magnification is 40×.  
Scale bars represent length of 100µm.

Author Manuscript

Author Manuscript

Author Manuscript

Author Manuscript

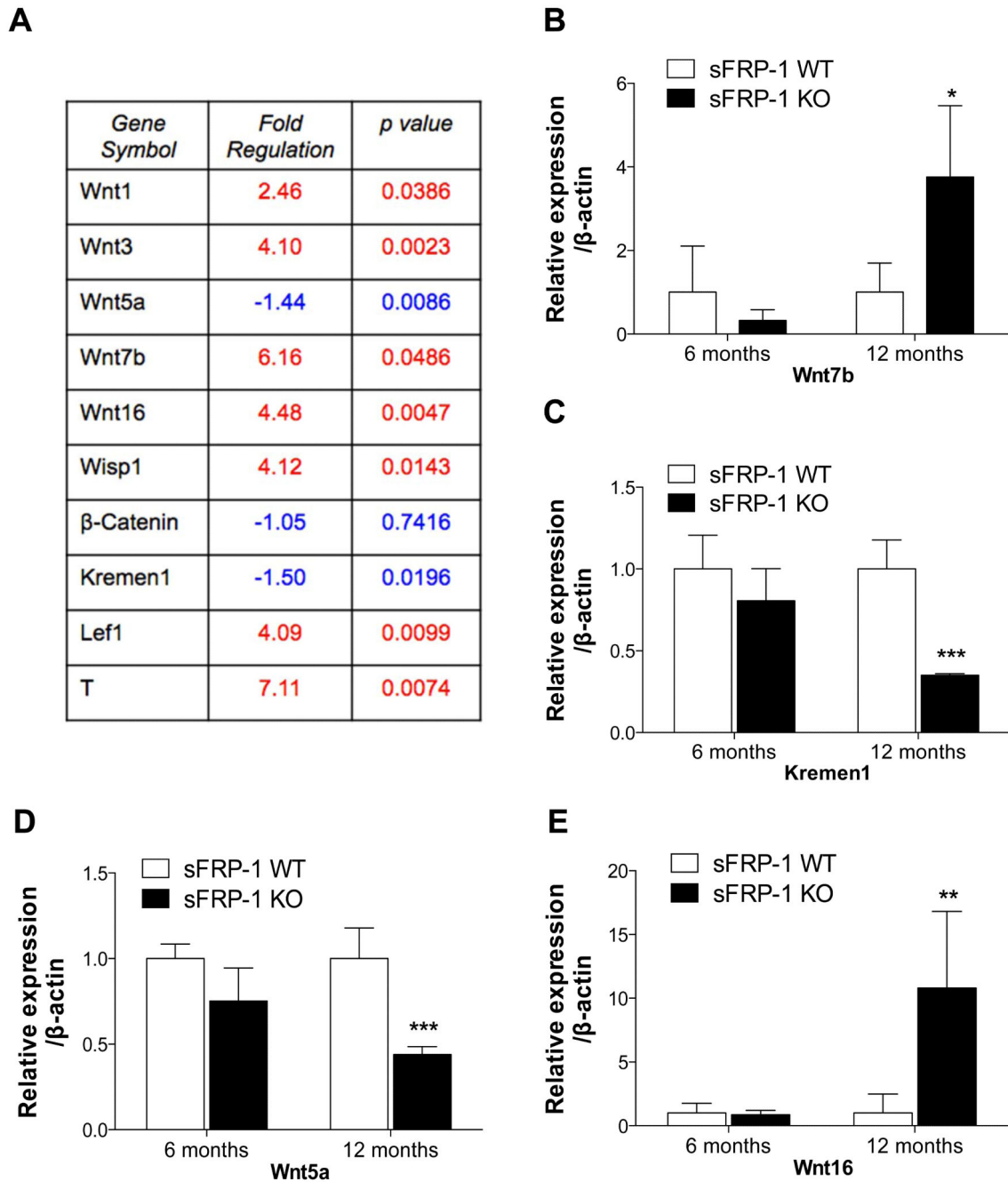


**Figure 5. Induction of Wnt signaling ligands in aged sFRP-1 KO hearts**

mRNA analysis of the Wnt target genes in the hearts of sFRP-1 WT and KO mice. (A) Wnt target gene array analysis (Sabiosciences). Selected genes expression relevant to canonical Wnt signaling pathway in 12 months old hearts of sFRP-1 WT and KO mice (n=3) were outlined in the table. Statistical analysis was done by Sabiosciences web-based software automatically. (B-E) Real Time PCR analysis confirmation of extracellular Wnt ligands such as (B) Wnt7b, (C) Kremen1, (D) Wnt5a, (E) Wnt16 in 6 and 12 months old hearts of sFRP-1 WT and KO mice (n=5).  $\beta$ -actin was used as a housekeeping control, data is

presented as fold of regulation. Significant differences were denoted by \* $P < 0.05$  or \*\* $P < 0.01$ , or \*\*\* $P < 0.001$ . > vs control littermate hearts. All values were expressed as mean  $\pm$  SEM.

Author Manuscript

Author Manuscript

Author Manuscript

Author Manuscript

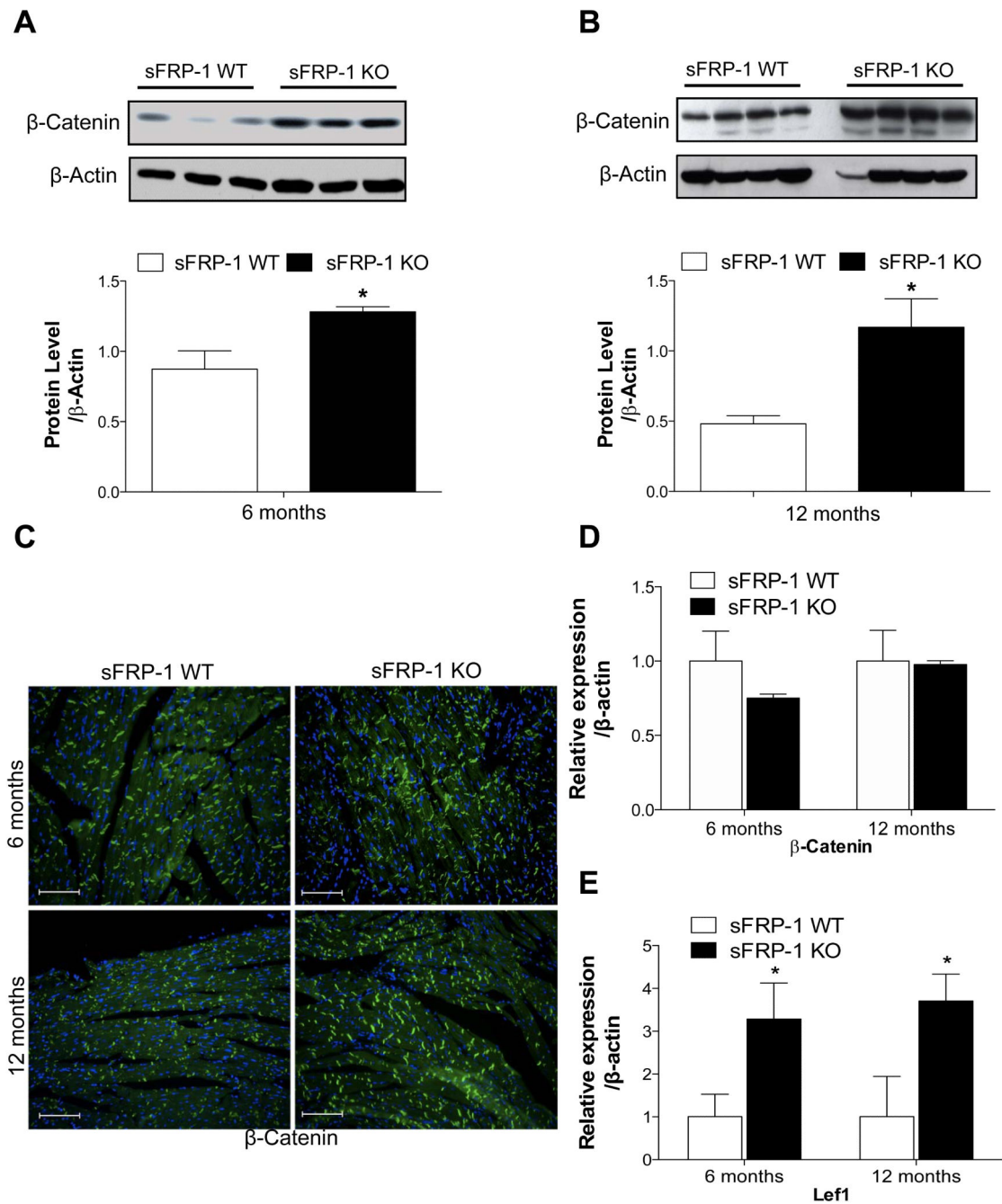


**Figure 6. Age-related increase in canonical Wnt signaling in sFRP-KO hearts**

(A-B) Protein expression of  $\beta$ -catenin analyzed by western blotting in control sFRP-1 WT hearts versus sFRP-1 KO hearts at 6 (A) and 12 (B) months of age.  $\beta$ -Actin was used as a housekeeping loading control. (C) Representative immunofluorescent staining for  $\beta$ -Catenin merged with DAPI in the myocardium of sFRP-1 KO compared with WT hearts at 6 and 12 months of age. Magnification is 20 $\times$ . Scale bars represent length of 100 $\mu$ m. (D-E) mRNA analysis of  $\beta$ -Catenin and Lef1 in sFRP-1 KO vs WT hearts at 6 and 12 months of age (n=5).  $\beta$ -actin was used as a housekeeping control, data is presented as fold of regulation.

Significant differences were denoted by \* $P < 0.05$  or \*\* $P < 0.01$ , or \*\*\* $P < 0.001$ . > vs control littermate hearts. All values were expressed as mean  $\pm$  SEM.

Author Manuscript

Author Manuscript

Author Manuscript

Author Manuscript

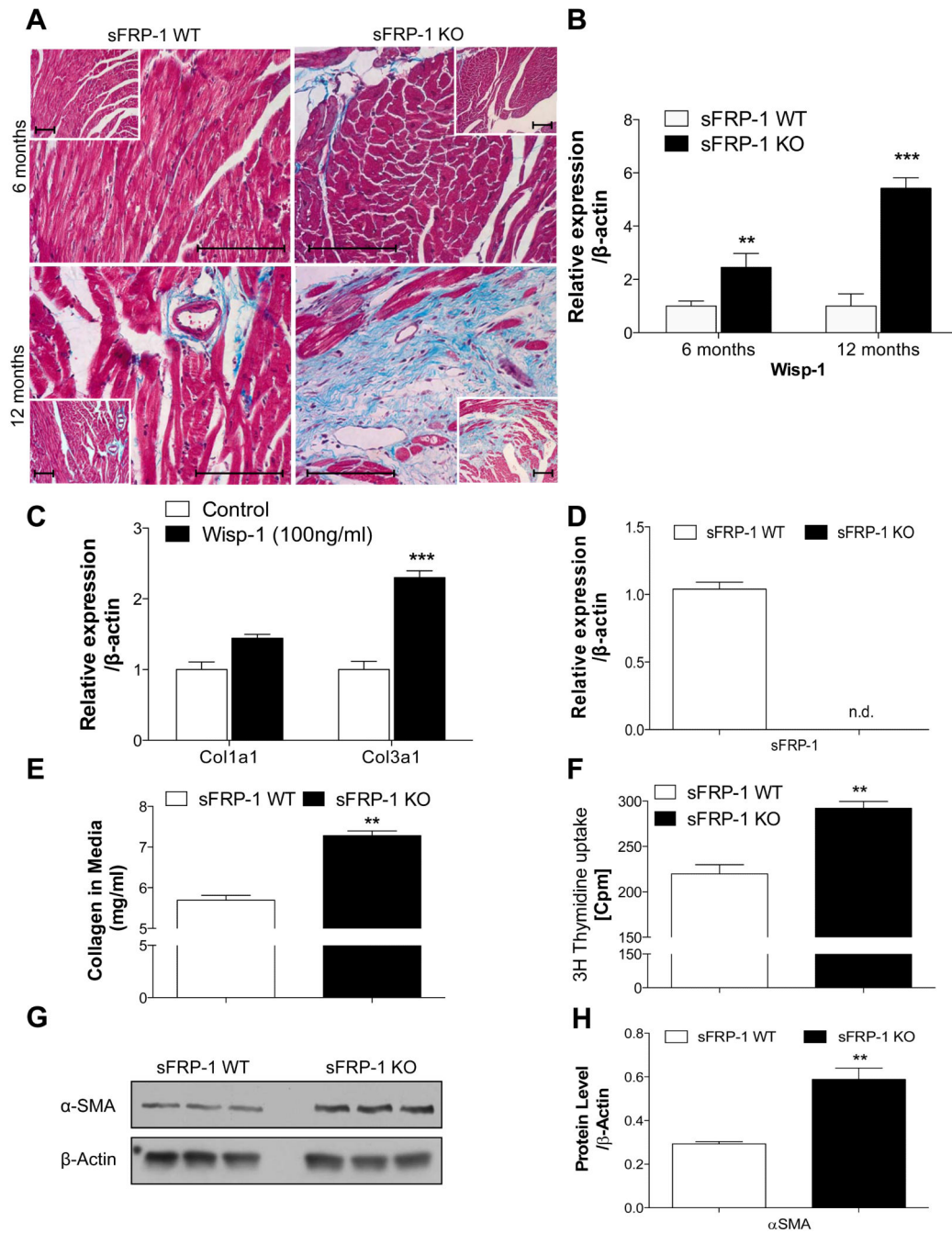


**Figure 7. Development of cardiac fibrosis in myocardium of aged sFRP-1 KO hearts**  
 (A) Representative pictures for Masson staining in the heart myocardium of sFRP-1 KO at 6 months or 12 months old mice vs WT littermates. Magnification is 40× and 20× (inset). Scale bars length is 100µm. (B) Wisp1 mRNA expression by Taqman Real-Time PCR in 6 and 12 months old sFRP-1 KO hearts in vs WT hearts (n=5). (C) Expression of collagens (1 and 3) in primary cardiac fibroblasts, isolated from sFRP-1 WT hearts (n=3). (D) mRNA expression of sFRP-1 in cardiac fibroblast (CF) isolated from sFRP-1 WT and KO mice (n=3). (E) Protein concentration of collagen in the media of sFRP-1 WT and KO fibroblasts

measured by Sircol assay (n=5). (F) Proliferation capacity of cardiac fibroblasts isolated from sFRP-KO mice vs WT mice measured by [<sup>3</sup>H]-Thymidine uptake (n=6). Values are expressed in [cpm-counts per minute] αSMA protein level in primary cardiac fibroblast isolated from sFRP-1 WT and KO mice analyzed by Western Blot (G) and subsequently quantified by densitometry (H). β-actin was used as a housekeeping control, data is presented as fold of regulation. Significant differences were denoted by \*P < 0.05 < or \*\*P < 0.01, or \*\*\*P < 0.001. > vs control littermate hearts. All values were expressed as mean ± SEM.

Author Manuscript

Author Manuscript

Author Manuscript

Author Manuscript

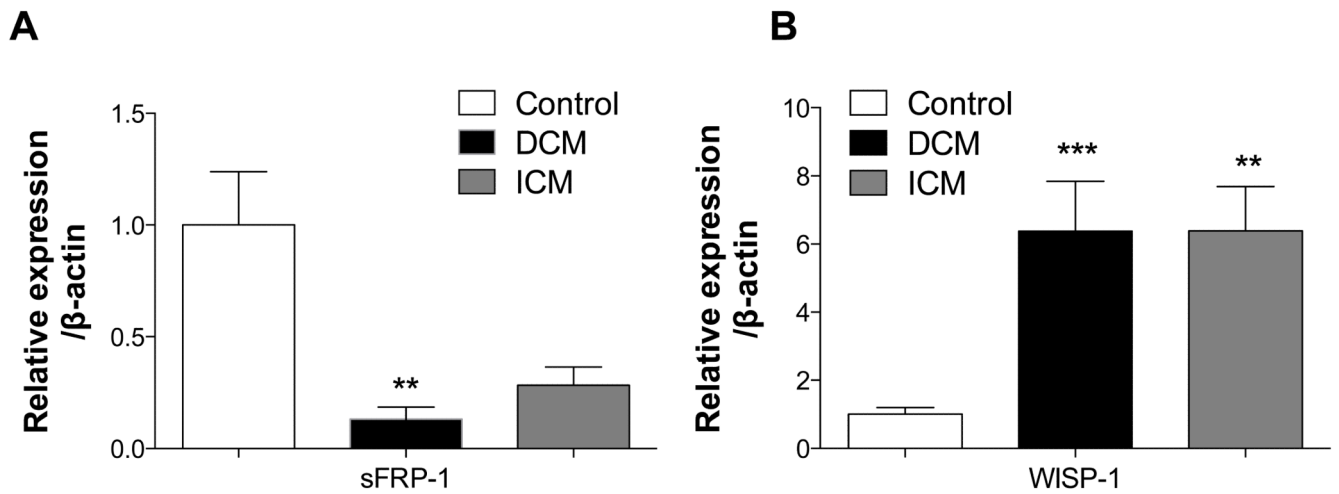


**Figure 8. Downregulation of sFRP-1 and upregulation of Wisp-1 in human dilated cardiomyopathy (DCM) and ischemic cardiomyopathy (ICM)**

(A) mRNA expression analysis of sFRP-1 and Wisp-1 in the heart left ventricles of Control patients (n=7) or in patients with DCM (n=8) and ICM (n=7). β-actin was used as a housekeeping control, data is presented as fold of regulation. Significant differences were denoted by \*P < 0.05 or \*\*P < 0.01, or \*\*\*P < 0.001. > vs control littermate hearts. All values were expressed as mean ± SEM.